Molecular Cytogenetics

RESEARCH

Open Access

Intrachromosomal insertion as a diagnostic challenge: a hidden structural rearrangement causing recurrent duplication and deletion

Rie Kawamura[1], Yui Shichiri[1], Hideki Suzuki[2], Yuri Murase[1,2], Yuki Naru[2], Tetsuaki Hara[3], Ayana Tsuboi[4], Hanae Satano[5], Eiji Sugihara[6] and Hiroki Kurahashi[1*]

Abstract

Background Intrachromosomal insertion is a rare form of structural chromosomal rearrangement that often cannot be accurately delineated by conventional G-banding, making it difficult to predict reproductive outcomes. In clinical practice, such insertions are often misinterpreted as inversions or remain undetected, leading to recurrent segmental imbalances in offspring. We aimed to characterize an unresolved structural rearrangement identified in a family and to clarify its reproductive implications through advanced cytogenetic and molecular analyses.

Methods Cytogenetic and molecular studies were conducted in a family where the proband exhibited a 17.8 Mb duplication at 9q21.31–q22.33. Although G-banding suggested a parental structural abnormality, its configuration could not be precisely defined. Subsequent preimplantation genetic testing for structural rearrangements (PGT-SR) using shallow whole-genome sequencing was performed on embryos, and further structural characterization was achieved through fluorescence in situ hybridization (FISH) and nanopore long-read sequencing.

Results PGT-SR identified recurrent segmental imbalances involving the same region as in the proband, including four duplications and one deletion among 13 embryos. FISH and long-read sequencing demonstrated that the paternal rearrangement represented an intrachromosomal inverted insertion, described as ins(9)(q34.13q22.33q21.31). The father was phenotypically normal but transmitted unbalanced gametes generated by recombination between the insertion and original sites, leading to recurrent chromosomal abnormalities.

Conclusions This case highlights the potential of intrachromosomal insertions, although balanced in carriers, to cause recurrent segmental duplications or deletions in offspring. Comprehensive analysis using FISH and long-read sequencing is essential for accurate diagnosis, appropriate genetic counseling, and informed reproductive decision-making.

Keywords Intrachromosomal insertion, Recurrent chromosomal imbalances, FISH, Long-read sequencing, PGT-SR

*Correspondence:
Hiroki Kurahashi
kura@fujita-hu.ac.jp
[1]Division of Molecular Genetics, Center for Medical Science, Fujita Health University, 1-98 Dengakugakubo, Kutsukake- cho, Toyoake 470-1192, Aichi, Japan
[2]OVUS Inc, Nagoya, Japan
[3]Division of Reproductive Medicine, Hiroshima Prefectural Hospital, Hiroshima, Japan
[4]Division of Pediatrics, Hiroshima Prefectural Hospital, Hiroshima, Japan
[5]Division of Genomic Medicine, Hiroshima Prefectural Hospital, Hiroshima, Japan
[6]Open Facility Center and Oncology Innovation Center, Research Promotion Headquarters, Fujita Health University, Toyoake, Japan

Introduction

The investigation of the etiology of phenotypes in pediatric genetics has evolved significantly over the past two decades, with chromosomal microarray analysis (CMA) now established as the first-tier diagnostic test for individuals with developmental disabilities or congenital anomalies [1]. CMA is increasingly performed in affected children to identify the underlying genetic cause, followed by parental G-banding for planning future pregnancies, reflecting advances in diagnostic approaches and the standardization of testing protocols [1, 2]. However, the resolution of G-banding is sometimes insufficient to obtain accurate information about structural abnormalities, complicating predictions of subsequent pregnancy outcomes.

The pathogenic interstitial copy number variants identified by CMA are generally *de novo*. However, parental analyses detect insertions in approximately 2.1% of cases [3]. Chromosomal insertions were previously referred to as insertional translocations; however, revisions to the International System for Human Cytogenomic Nomenclature (ISCN) have clarified that the insertion of a chromosomal segment into a breakpoint within the same chromosome or into a different chromosome is to be classified as an *insertion*, distinct from translocations. Identification of a parental insertion is clinically important because of its implications for recurrence risk in subsequent offspring. While interchromosomal insertions can usually be recognized relatively easily by conventional cytogenetic techniques, intrachromosomal insertions are far more difficult to detect. In particular, when an insertion occurs close to its origin or in an inverted orientation, the banding pattern may change so extensively that its origin cannot be determined with confidence. In some cases, intrachromosomal insertions have been mistaken for paracentric inversions [4, 5]. Given the substantial differences in reproductive consequences between insertions and inversions, an accurate diagnosis is essential. In intrachromosomal insertions, meiotic recombination between the insertion site and the original site can lead to gametes carrying duplications or deletions of the inserted segment, resulting in a high recurrence risk for chromosomal imbalances in offspring [6, 7]. In contrast, in paracentric inversions, crossing over within the inverted segment results in the formation of acentric fragments and dicentric chromosomes, which generally have a negligible impact on reproduction [8, 9]. Although the distinction between these two types of rearrangements is crucial for accurate genetic counseling and reproductive planning, conventional G-banding analysis often cannot differentiate between them, leading to inappropriate counseling and suboptimal management strategies [10].

In this report, we present a case that exemplifies these diagnostic challenges and highlights the importance of precise structural characterization. We encountered a family with a 17.8 Mb duplication at 9q21.31–q22.33 in a proband. Paternal G-banding revealed a structural abnormality suggestive of either an inversion or an insertion, but the analysis was unable to distinguish between these abnormalities. A combination of targeted fluorescence in situ hybridization (FISH) analysis and long-read sequencing demonstrated that the paternal rearrangement was an intrachromosomal inverted insertion. This precise characterization enabled evidence-based genetic counseling and informed reproductive decision-making, underscoring the critical importance of molecular approaches in defining chromosomal structural abnormalities.

Materials and methods

Case

The male proband was the first child of a nonconsanguineous, healthy couple with no family history of genetic disorders or birth defects. He was delivered at term with a birth weight of 2286 g (– 2.2 SD), classified as low birth weight, and had Apgar scores of 9 at both 1 and 5 min. He was diagnosed with congenital hypothyroidism and has since been treated with thyroid hormone replacement therapy. At 3 months of age, he presented with projectile vomiting and failure to thrive, requiring nasogastric feeding, although no gastrointestinal malformation was identified. To investigate the etiology of this clinical presentation, including developmental delay and dysmorphic features, G-banding karyotype analysis was performed. This analysis identified an abnormal chromosome 9 with additional material at the terminal region of the long arm, which was reported as 46,XY,add(9)(q34) (Supplementary Figure S1A, left).

To further characterize this abnormality, CMA was performed, which confirmed that the additional material represented a duplication of the corresponding 17.8 Mb region; arr[GRCh37] 9q21.31q22.33(82,907,524_100,663,735)x3 (Supplementary Figure S1A, right). Subsequent parental G-banding studies identified a structural rearrangement in the corresponding region of chromosome 9 in the father (Supplementary Figure S1B, left); the mother's karyotype was normal (46,XX). Based on the G-banding pattern and additional FISH analysis, the father's karyotype was reported as 46,XY, der(9)(pter→q21::?::q34→qter).ish der(9)(wcp9+,subtel9q+) (Supplementary Figure S1B, right).

Although an inversion or insertion was suspected based on the conventional understanding of recombination within a paracentric inversion loop (u-loop recombination), the precise nature of the rearrangement remained unclear [9, 11]. In anticipation of a subsequent

pregnancy and to avoid recurrence in future offspring, the couple requested preimplantation genetic testing for structural rearrangements (PGT-SR). After obtaining written informed consent, blood samples were collected from the father. Genomic DNA was extracted using standard procedures. This study was approved by the Institutional Ethical Review Board of Fujita Health University (approval number HG24-017).

PGT-SR

Diagnostic PGT-SR was performed using whole-genome amplification (WGA) DNA obtained from trophoectoderm (TE) cells via blastocyst biopsy from 5-day embryos. We used the ReproSeq™ PGS kit for chromosomal copy number analysis. Library preparation for NGS analysis was conducted in accordance with the manufacturer's protocol. Shallow whole-genome sequencing (WGS) for robust copy number profiling was conducted using the Ion Chef equipment and the Ion S5 sequencer (Thermo Fisher Scientific, Waltham, MA). Copy numbers were evaluated using the IonReporter system.

FISH

To clarify the structure of the father's der(9), we performed two-color FISH analyses using bacterial artificial chromosome (BAC) probes. BAC clones were selected from the BACPAC Resources Center (Children's Hospital Oakland Research Institute, Oakland, CA) based on the microarray results from the proband. The probes were designed to investigate both the structure and orientation of the rearranged segment. BAC DNA was extracted using the NucleoBond BAC 100 Kit (Macherey-Nagel, Düren, Germany) and labeled by nick translation using either SpectrumGreen-dUTP or SpectrumRed-dUTP (Abbott Molecular, Des Plaines, IL).

Metaphase chromosome preparations were obtained from peripheral blood lymphocytes following established protocols. FISH was performed according to standard procedures. Briefly, slides containing metaphase spreads were denatured in 70% formamide/2× SSC at 73 °C for 3 min, dehydrated in an ethanol series (70%, 85%, and 100%), and then air-dried. The labeled probes were denatured at 73 °C for 5 min before being applied to the slides. Hybridization was conducted overnight at 37 °C in a humidified chamber. Post-hybridization washes were performed in 0.4× SSC/0.3% NP-40 at 73 °C for 2 min, followed by washes in 2× SSC/0.1% NP-40 at room temperature for 1 min. The slides were counterstained with DAPI (4′,6-diamidino-2-phenylindole) and analyzed using a fluorescence microscope (Zeiss, Oberkochen, Germany) equipped with appropriate filter sets. A minimum of 20 metaphase spreads were analyzed for each FISH experiment, and images were captured using ISIS software (Metasystems, Altlussheim, Germany).

Long-read sequencing for breakpoint analysis

To precisely determine the breakpoints of the structural rearrangement in the father, we performed long-read sequencing using the Oxford Nanopore Technologies platform (Oxford Nanopore Technogies, Oxford, UK). High-molecular-weight genomic DNA was extracted from the father's peripheral blood using the MagAttract HMW DNA Kit (Qiagen, Venlo, Netherlands). The quality and quantity of the extracted DNA were assessed using a NanoDrop spectrophotometer (Thermo Fisher Scientific) and a Qubit fluorometer (Thermo Fisher Scientific). Library preparation was performed using the Ligation Sequencing Kit (SQK-LSK109, Oxford Nanopore Technologies) according to the manufacturer's protocol. Briefly, 1 μg of high-molecular-weight DNA was repaired and end-prepped using the NEBNext FFPE DNA Repair Mix and the NEBNext Ultra II End Repair/dA-Tailing Module (New England Biolabs, Ipswich, MA). Adapter ligation was performed using the NEBNext Quick Ligation Module (New England Biolabs) and Oxford Nanopore Technologies–specific adapters.

The prepared library was loaded onto a FLO-MIN106 R9.4.1 flow cell (Oxford Nanopore Technologies) and sequenced on a GridION device (Oxford Nanopore Technologies) for 48 h. Adaptive sampling was carried out using the MinKNOW software feature, targeting the entire long arm of chromosome 9 (chr9:46,267,186 – 150,617,247; T2T reference). Base calling was performed using Guppy v5.0.7 with the high-accuracy model. Sequence alignment was performed using minimap2 v2.17 with the map-ont preset to the T2T (Telomere-to-Telomere) reference genome. Structural variant calling was conducted using Sniffles v1.0.12 with a minimum support of 10 reads for variant calls. SURVIVOR v1.0.7 was used to merge and filter structural variants. Breakpoint analysis was performed using Integrative Genomics Viewer (IGV) to visualize and precisely identify the chromosomal breakpoints of the rearrangement on chromosome 9.

Results

PGT-SR identification of recurrent duplications and deletions

Because the father of the proband had a structural abnormality involving the same chromosomal region duplicated in the proband, the couple underwent PGT-SR for their subsequent pregnancy to avoid recurrence of the cytogenetic abnormality observed in the proband, although the exact rearrangement in the father remained undefined. A TE biopsy was performed on 13 blastocysts, and copy number analysis via shallow WGS revealed two embryos with euploidy, six embryos with aneuploidy, four embryos with the same duplication as in the proband, and one embryo with a deletion at the identical

locus (Fig. 1). Based on these findings, the father's der(9) was likely to be an intrachromosomal insertion rather than a paracentric inversion. It was presumed that the proband originated from a paternal gamete carrying a recombinant chromosome formed between the original and recipient sites of the insertion.

FISH characterization of the intrachromosomal inverted insertion

To clarify the structure of the father's der(9), we performed two-color FISH in three different patterns. The first FISH experiment was aimed at distinguishing between a paracentric inversion and an intrachromosomal insertion. We designed probes targeting regions flanking the duplicated segment identified in the proband: the proximal region (9q21.2; RP11-498N2) and the distal region (9q22.33; RP11-106N7). If it were a paracentric inversion, the two-color signals would be more separated than normal. In contrast, if it were an insertion, the signals would be closer together than normal and appear adjacent (Fig. 2A). FISH revealed that the distance between the two signals was shorter than that observed on the normal chromosome, indicating that the father's der(9) represented an insertion of a proximal segment into a distal site on the same chromosome rather than a paracentric inversion (Fig. 2A).

Next, we investigated where on 9q the insertion had occurred. Previous FISH analysis had revealed that the 9q subtelomeric region of der(9) was intact, and G-banding suggested that a breakpoint was located in the 9q34 region. We designed probes targeting the 9q34 region using 9q34.11 (RP11-88L8), 9q34.13 (RP11-203M2), and 9q34.3 (RP11-216L13). The signals on both 9q34.11 (data not shown) and 9q34.13 were more separated than on the normal chromosome 9, revealing that the insertion had occurred between 9q34.13 and 9q34.3 (Fig. 2B).

We then examined the orientation of the inserted fragment by designing probes within the duplicated region of the proband: 9q21.31 (RP11-289F5) and 9q22.33 (RP11-23B15). The results showed that the signal orientation on der(9) was inverted compared to the normal chromosome 9, confirming that this was an inverted insertion (Fig. 2C). Based on these FISH results, the father's structural abnormality was determined to be an intrachromosomal inverted insertion rather than a paracentric inversion.

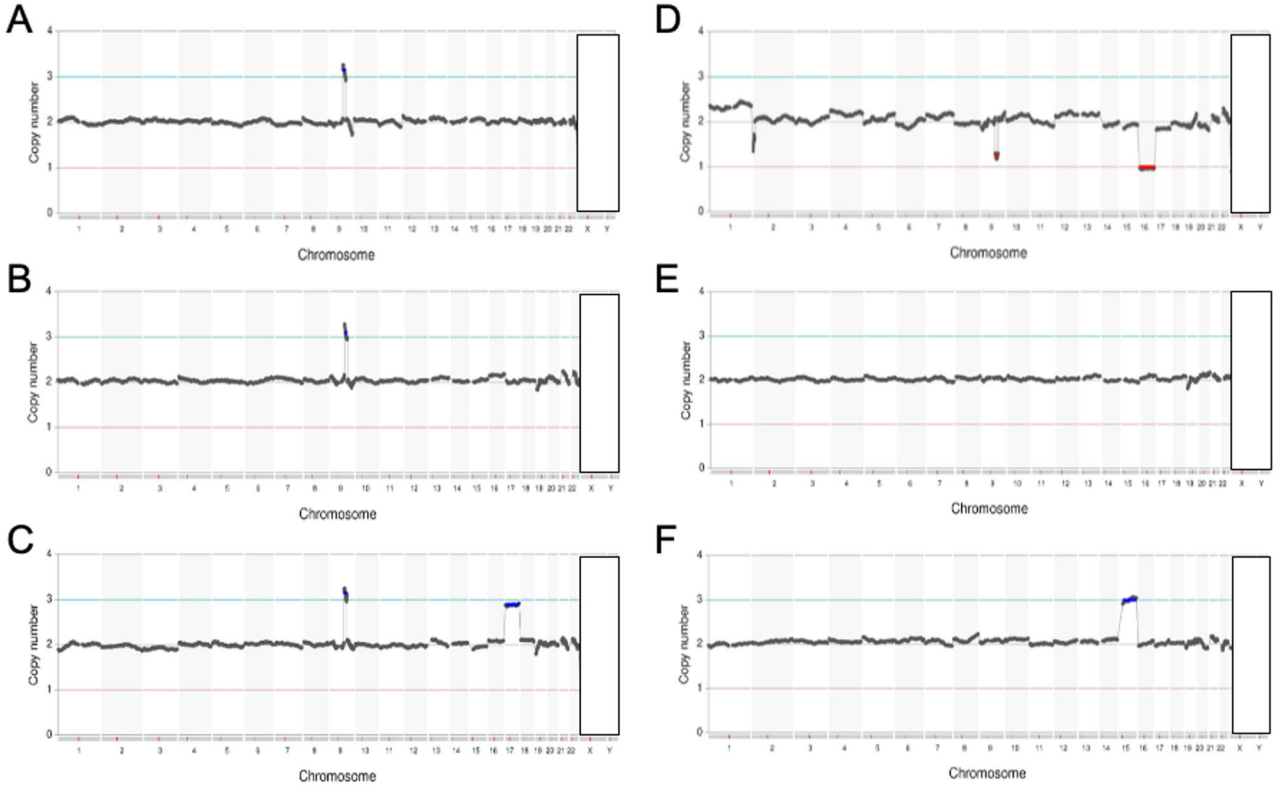

Fig. 1 Representative idiogram of PGT-SR of the parents. Out of 13 embryos, 4 showed duplications while 1 showed a deletion in the 9q21.31-q22.33 region, similar to that identified in the proband. **A–C**, duplication; **D**, deletion; **E**, euploid; **F**, aneuploid unrelated to the father's der(9). Data on the sex chromosomes of each embryo was masked for confidentiality (white boxes)

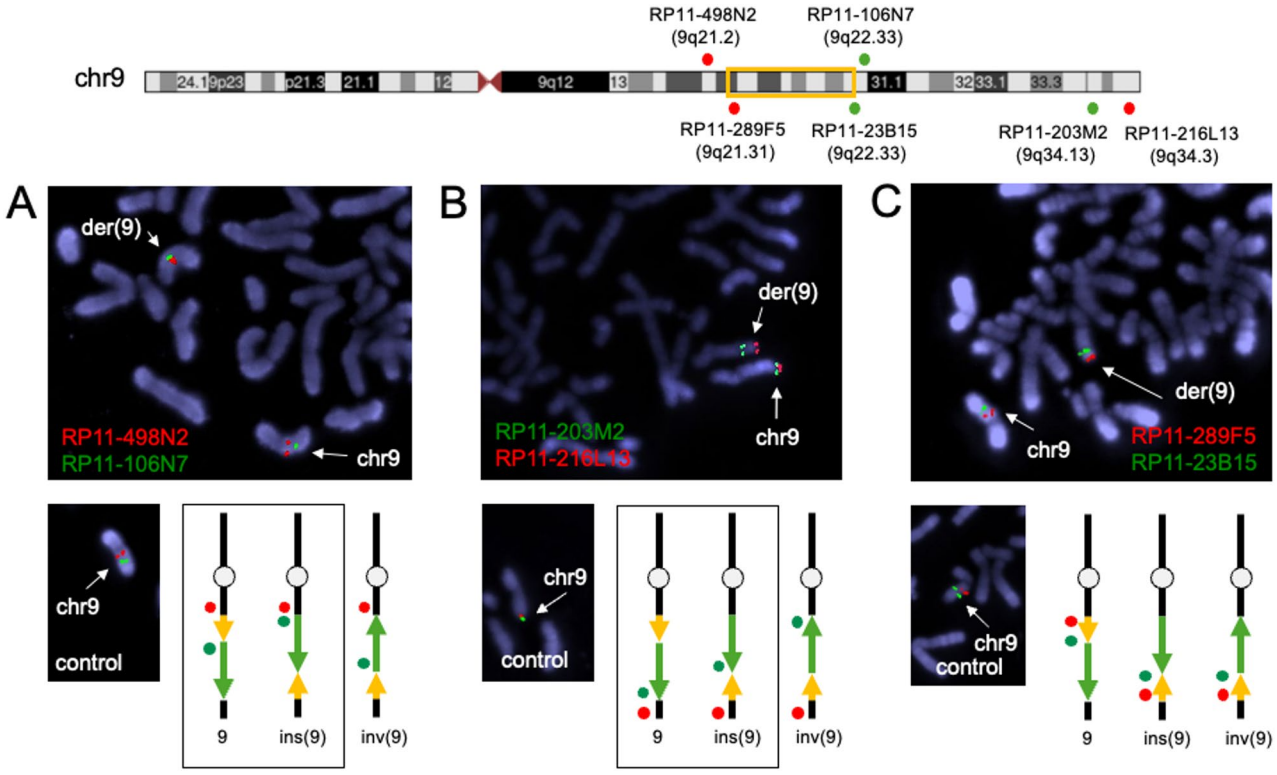

Fig. 2 Metaphase FISH analysis to determine the structural abnormality in the father's der(9). The upper panel shows the overall map of BAC probes used in this study on chromosome 9. The duplicated segment is indicated by a yellow box. **(A)** Distinction between paracentric inversion and intrachromosomal insertion. Two-color FISH using probes flanking the duplicated segment: RP11-498N2 (9q21.2, red) and RP11-106N7 (9q22.33, green). FISH images show the father's normal chromosome 9 and der(9). Schematic diagrams illustrate the expected signal patterns for normal chromosome 9, ins(9), and inv(9) configurations. In der(9), adjacent red and green signals were observed, indicating an intrachromosomal insertion rather than a paracentric inversion. The yellow arrows indicate the putative insertion segment, while the green arrows indicate the genomic region between the original site and the site of the insertion. **(B)** Identification of the recipient site. Two-color FISH using probes targeting the 9q34 region: RP11-203M2 (9q34.13, green) and RP11-216L13 (9q34.3, red). FISH images illustrate the increased distance between the green signals at 9q34.13 compared to the normal chromosome 9, revealing that the insertion occurred between 9q34.13 and 9q34.3. **(C)** Determination of the orientation of the inserted fragment. Two-color FISH using probes within the duplicated region: RP11-289F5 (9q21.31, red) and RP11-23B15 (9q22.33, green). FISH images show that the signal orientation on der(9) was inverted compared to the normal chromosome 9, indicating an inverted insertion. Chromosomes were counterstained with DAPI (blue). Arrows indicate the normal and derivative chromosomes 9 in each panel

Breakpoint analysis using long-read sequencing

To precisely determine the breakpoints of the structural rearrangement, we performed long-read sequencing of the father's genomic DNA using the Oxford Nanopore Technologies GridION platform with adaptive sampling targeting the entire long arm of chromosome 9 (chr9:46,267,186 – 150,617,247; T2T reference). Structural variant analysis and subsequent visual inspection in IGV identified three breakpoints associated with the rearrangement, which were mapped to the T2T reference genome (Fig. 3A). The three breakpoints were identified with cuts occurring at 92,433,662–92,433,663 in 9q21.31, at 110,097,716–110,097,717 in 9q22.33, and at 148,641,476–148,641,477 in 9q34.13. The first breakpoint (BP1) was located at position 92,433,662 in 9q21.31, corresponding to the proximal boundary of the inserted segment. The second breakpoint (BP2) was located at position 110,097,716 in 9q22.33, representing the distal boundary of the inserted segment. The third breakpoint (BP3) was located at position 148,641,476 in 9q34.13, indicating the recipient site. Detailed analysis of the breakpoint junctions using nanopore sequencing confirmed that the father's der(9) represented an intrachromosomal inverted insertion, consistent with the FISH findings. The BP1–BP2 fragment from 9q21.31 to 9q22.33 was inserted in reverse orientation into BP3 at 9q34.13, which can be designated as ins(9)(q34.13q22.33q21.31), that is, ins(9)(pter→q21.31::q22.33→q34.13::q22.33→q21.31::q34.13→qter).

BP1 and BP2 did not disrupt any functional genes, whereas BP3 was located within the *PMPCA* gene, which is a causative gene for spinocerebellar ataxia, autosomal recessive 2 (SCAR2, OMIM #213200). Since SCAR2 is an early childhood-onset neurologic disorder, the father is a healthy carrier of this autosomal recessive condition. According to the ClinGen and DECIPHER databases,

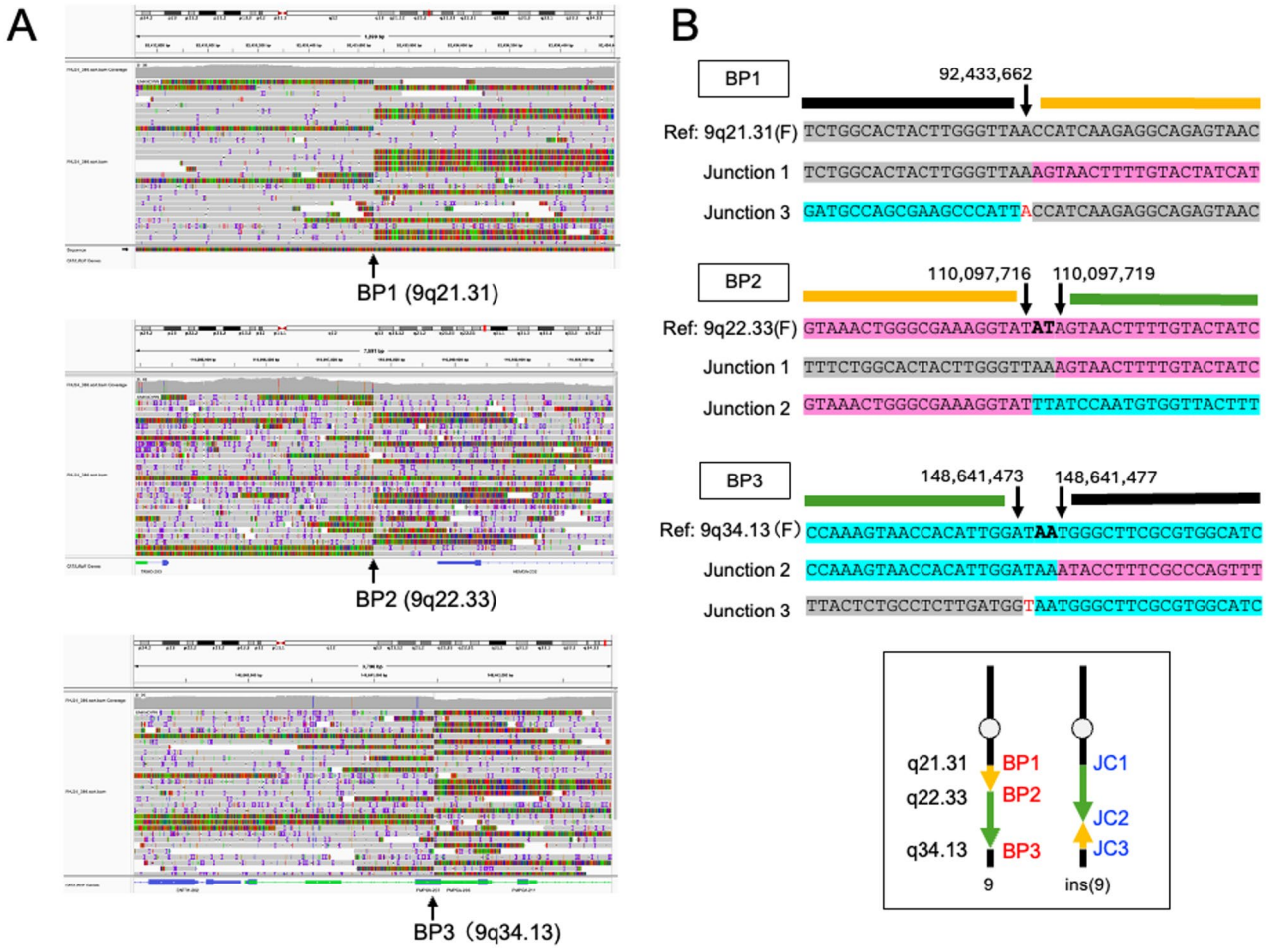

Fig. 3 Nanopore sequence analysis to determine the structural abnormality in the father's der(9). **(A)** IGV plot of the regions encompassing the three breakpoints on chromosome 9q. **(B)** Alignment of the breakpoint sequences with junction sequences. The original sequences for BP1, BP2, and BP3 are indicated by grey, pink, and blue, respectively. The yellow bars indicate the insertion segment, while the green bars indicate the genomic region between the original site and the site of the insertion. The 2-bp microdeletion and 2-bp microduplication identified at the breakpoints are bolded, while the microhomology at junction 3 is indicated in red

BP1-BP2 segment contains 89 genes, including 22 OMIM morbid genes. Among these, *HNRNPK* and *PTCH1* have sufficient evidence for haploinsufficiency based on ClinGen dosage sensitivity scores, and deletions involving this region are therefore expected to result in a clinical phenotype. In contrast, the proband carried a duplication of the BP1–BP2 segment, for which no genes have been assigned established triplosensitivity scores.

All three breakpoints were located in regions devoid of sequence motifs commonly associated with genomic instability, including interspersed repetitive elements, tandem repeats (e.g., microsatellites), and palindromic or inverted repeat sequences. Junction analysis at the nucleotide level revealed specific breakpoint connections: JC1 connected 92,433,662::110,097,719, JC2 connected 148,641,476::110,097,716, and JC3 connected 92,433,663::148,641,474 (Fig. 3B). BP1 is a simple breakage, BP2 is accompanied by the deletion of two nucleotides (AT), and BP3 is associated with the duplication of two nucleotides (AA). Both JC1 and JC2 were rejoined with blunt ends, possibly via non-homologous end joining (NHEJ), while JC3 contained one identical nucleotide at the point where the original two sequences were joined to form a hybrid representing microhomology-mediated end joining (MMEJ). Based on comprehensive cytogenetic analysis, the father's structural abnormality was characterized as follows according to the ISCN 2024: 46,XY,ins(9)(q34.13q22.33q21.31).ish ins(9)(wcp9+,subtel9q+).seq[T2T-CHM13v2.0] ins(9)(pter→q21.31::q22.33→q34.13::q22.33→q21.31::q34.13→qter) CHM13#chr9:g.[92433663_110097716del;148641473_148641474ins[92433663_110097716inv].

Taken together, the father was found to carry an intrachromosomal inverted insertion designated ins(9)(pter→q21.31::q22.33→q34.13::q22.33→q21.31::q34.13→qter). The proband and the embryos with a deletion or

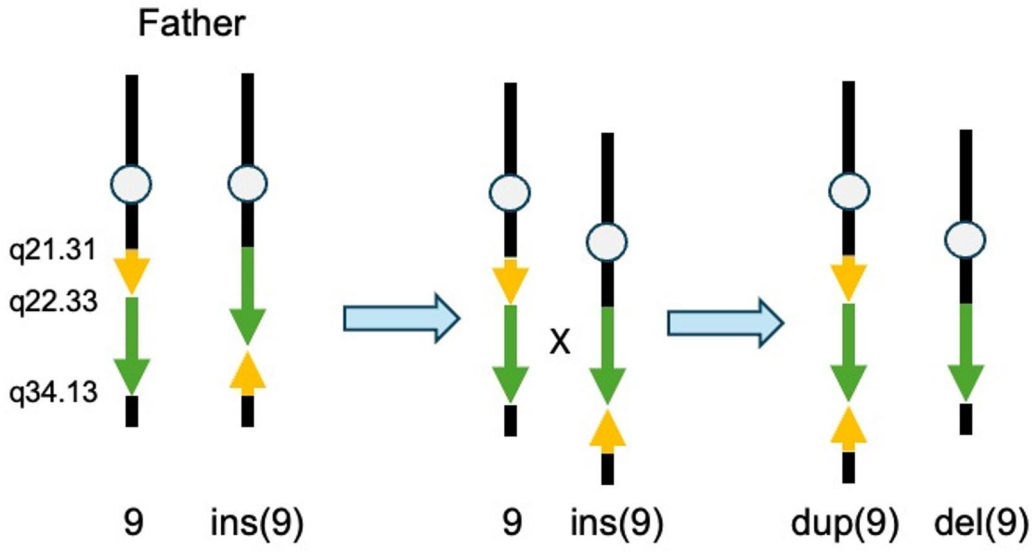

Fig. 4 The mechanism underlying the formation of the chromosomal structural abnormalities in this family is thought to result from recombination within the ins(9) region, generating gametes with interstitial duplication dup(9) where the inserted fragment is duplicated and interstitial deletion del(9) where the inserted fragment is deleted. The affected child who showed a gain of 9q21.31→q22.33 inherited dup(9). Embryos with partial trisomy of 9q21.31→q22.33 identified by PGT-SR inherited dup(9), while embryos with partial monosomy of 9q21.31→q22.33 identified by PGT-SR inherited del(9). The yellow arrows indicate the inverted insertion segment, while the green arrows indicate the genomic region between the original site and the site of the insertion

duplication at the same region were presumed to have originated from a paternal gamete harboring a recombinant chromosome formed between the original and recipient sites of the insertion (Fig. 4).

Discussion

Among the various types of structural rearrangements, intrachromosomal insertions and paracentric inversions present particular diagnostic challenges, as they are often indistinguishable by conventional G-banding analysis alone [10]. Although these rearrangements are difficult to detect and differentiate using G-banding, they have dramatically different recurrence risks for unbalanced offspring and implications for reproduction and genetic counseling. In paracentric inversions, meiotic recombination within the inverted segment results in the formation of acentric fragments and dicentric chromosomes, which generally have negligible impact on reproductive outcomes [8, 9]. However, in intrachromosomal insertions such as in this case, meiotic recombination between the insertion site and the original site leads to gametes carrying duplications or deletions of the inserted segment, resulting in a high recurrence risk for chromosomal imbalances in offspring [6, 7]. In the present case, although the G-banding results were inconclusive, the couple opted for PGT-SR, which allowed the identification of embryos with deletions or duplications and thus averted unfavorable outcomes. Nonetheless, it is crucial to definitively distinguish between paracentric inversion and intrachromosomal insertion prior to reproductive planning, as this distinction provides the foundation and motivation for informed decision-making regarding PGT-SR [12].

As a diagnostic approach, the combination of metaphase FISH analysis and long-read sequencing proved to be highly effective for distinguishing intrachromosomal insertions and paracentric inversions. FISH analysis was essential for identifying intrachromosomal insertions, including both the original site and recipient site, and further for confirming the orientation of the inserted segment. Although FISH remains a valuable and widely used technique, it requires the formulation of an appropriate working hypothesis and the careful selection and preparation of multiple probes targeting the relevant chromosomal regions. In the present case, the breakpoint structure was relatively simple, allowing clear interpretation by FISH. However, in more complex rearrangements, FISH alone may not provide sufficient resolution to define the exact configuration. In such instances, nanopore long-read sequencing would offer a more reliable and informative approach. In the present case, nanopore sequencing with adaptive sampling targeting chromosome 9q provided sufficiently high resolution for breakpoint analysis. The use of the T2T reference genome enhanced the accuracy of the mapping and junction characterization. This approach enabled us to overcome the limitations of conventional cytogenetic methods and achieve nucleotide-level precision in

structural variant analysis [13]. Even in more complex rearrangements, nanopore sequencing can provide sufficient resolution to define the exact configuration of complicated rearrangements.

Although insertions, whether interchromosomal or intrachromosomal, appear cytogenetically to involve only three breakpoints, they often exhibit far more complex structures at the molecular level [14, 15]. The breakpoints may undergo chromothripsis-like fragmentation, followed by intricate reassembly that often results in the loss of small genomic fragments that fail to rejoin. In our case, however, the rearrangement was exceptionally simple, consisting of only three breakpoints and a misrepair event consistent with the microscopic findings. Because no fragments were lost and the rearrangement was fully balanced, the father was completely healthy, although the rearrangement did result in reproductive difficulties. When an insertion is identified in an asymptomatic parent during the evaluation of a child carrying a pathogenic copy number variation, it is likely that such an insertion, whether interchromosomal or intrachromosomal, has a similarly simple structure.

The molecular mechanism underlying the intrachromosomal inverted insertion found in the father remains uncertain. None of the three breakpoint regions exhibited sequence features typically associated with genomic fragility, such as gene-dense segments, high densities of repetitive elements, tandem repeats, or palindromic sequences. Accordingly, there was no clear explanation for why the DNA breaks occurred. Whether the initiating lesions were triggered by exogenous insults or by endogenous events such as replication stalling could not be determined. However, the available evidence suggests that the insertion likely arose from a stochastic, nonspecific DNA breakage event. The subsequent misrepair is most plausibly attributable to NHEJ or MMEJ, mechanisms commonly implicated in the formation of insertions [14, 15]. Even in far more complex chromosomal rearrangements, similar breakpoint characteristics have been described, and their detailed origins remain unresolved [16]. More recently, an intriguing model has been proposed in which breakpoints of complex structural variants correlate with the distribution of ATAC-seq reads in mature sperm, suggesting that *de novo* DNA breaks preferentially arise in chromatin regions not protected by histones. These lesions may then be erroneously rejoined after fertilization through NHEJ or MMEJ, ultimately generating complex rearrangements [17]. Further genomic and epigenomic characterization of breakpoint architecture, such as in the present case, will be essential for elucidating the mechanisms responsible for these structural abnormalities.

Conclusion

This study underscores the importance of comprehensive structural characterization in couples with reproductive failure or affected offspring. The father's balanced intrachromosomal insertion, undetectable by conventional karyotyping, had a significant impact on reproductive outcomes. The combined use of FISH and long-read sequencing proved to be a powerful strategy for accurately resolving the structural complexity and elucidating the mechanisms underlying the recurrent interstitial deletions and duplications within the family. Such detailed breakpoint characterization enables the precise application of PGT-SR, facilitating the identification of unbalanced embryos and improving the likelihood of achieving chromosomally normal offspring. These findings highlight the need to integrate advanced cytogenetic and molecular techniques into clinical practice to ensure accurate diagnosis, effective genetic counseling, and optimal reproductive outcomes for families with structural chromosomal rearrangements.

Abbreviations

FISH	Fluorescence in situ hybridization
PGT-SR	Preimplantation genetic testing for structural rearrangements
CMA	Chromosomal microarray analysis
BAC	Bacterial artificial chromosome
NHEJ	Non-homologous end joining
MMEJ	Microhomology-mediated end joining

Supplementary Information

The online version contains supplementary material available at https://doi.org/10.1186/s13039-026-00748-5.

Supplementary Material 1.

Acknowledgements

We thank the patients and their family members for participating in this study.

Author contributions

Study concepts: RK, HK; Collection of patient data: TH, AT, HSatano; PGT-SR: HSuzuki, YM, HK; Karyotyping, FISH and interpretation: YN, RK; Long-read sequencing: RK, YS, ES, HK; manuscript preparation: RK, HK. All authors read and approved the final version of the manuscript.

Funding

This work was supported by JSPS KAKENHI Grant Number JP23K06619.

Data availability

Please contact the corresponding author regarding any data requests.

Declarations

Ethics approval and consent to participate

This study was approved by Fujita Health University Ethics Committee (approval number HG24-017). Written informed consent for participation in the study was obtained from the patient's legal guardians and all adult participants.

Consent for publication

Written informed consent was obtained from the patient's legal guardians and the patient's father for publication of this study.

Competing interests
The authors declare no competing interests.

Received: 25 November 2025 / Accepted: 18 January 2026
Published online: 25 January 2026

References

1. Miller DT, Adam MP, Aradhya S, Biesecker LG, Brothman AR, Carter NP, et al. Consensus statement: chromosomal microarray is a first-tier clinical diagnostic test for individuals with developmental disabilities or congenital anomalies. Am J Hum Genet. 2010;86:749–64. https://doi.org/10.1016/j.ajhg.2010.04.006.
2. Ahn JW, Bint S, Bergbaum A, Mann K, Hall RP, Ogilvie CM. Array CGH as a first line diagnostic test in place of karyotyping for postnatal referrals - results from four years' clinical application for over 8,700 patients. Mol Cytogenet. 2013;6(1):16. https://doi.org/10.1186/1755-8166-6-16.
3. Nowakowska BA, de Leeuw N, Ruivenkamp CA, Sikkema-Raddatz B, Crolla JA, Thoelen R, et al. Parental insertional balanced translocations are an important cause of apparently de novo CNVs in patients with developmental anomalies. Eur J Hum Genet. 2012;20(2):166–70. https://doi.org/10.1038/ejhg.2011.157.
4. Madan K, Menko FH. Intrachromosomal insertions: a case report and a review. Hum Genet. 1992;89(1):1–9. https://doi.org/10.1007/BF00207032.
5. Ardalan A, Prieur M, Choiset A, Turleau C, Goutieres F, Girard-Orgeolet S. Intrachromosomal insertion mimicking a pericentric inversion: molecular cytogenetic characterization of a three break rearrangement of chromosome 20. Am J Med Genet A. 2005;138A(3):288–93. https://doi.org/10.1002/ajmg.a.30966.
6. Van Hemel JO, Eussen HJ. Interchromosomal insertions. Identification of five cases and a review. Hum Genet. 2000;107:415–32. https://doi.org/10.1007/s004390000398.
7. Kang SH, Shaw C, Ou Z, et al. Insertional translocation detected using FISH confirmationof array-comparative genomic hybridization (aCGH) results. Am J Med Genet A. 2010;152A(5):1111–26. https://doi.org/10.1002/ajmg.a.33278.
8. Kaiser P. Pericentric inversions: problems and significance for clinical genetics. Hum Genet. 1984;68:1–47. https://doi.org/10.1007/BF00293869.
9. Madan K. Paracentric inversions: a review. Hum Genet. 1995;96(5):503–15. https://doi.org/10.1007/BF00197403.
10. Madan K, Nieuwint AW. Reproductive risks for paracentric inversion heterozygotes: inversion or insertion? That is the question. Am J Med Genet. 2002;107(4):340–3. https://doi.org/10.1002/ajmg.10173.
11. Paskulin GA, Riegel M, Machado Rosa RF, Graziadio C, Gazzola Zen PR. Interstitial deletion of 7q31.32 q33 secondary to a paracentric inversion of a maternal chromosome 7. Eur J Med Genet. 2011;54(2):181–5. https://doi.org/10.1016/j.ejmg.2010.10.012.
12. Zhang Z, Luo K, Zhang S, Cheng D, Hu L, Tan YQ, et al. Clinical outcomes in carriers of insertional translocation: a retrospective analysis of comprehensive chromosome screening results. F S Rep. 2023;5(1):55–62. https://doi.org/10.1016/j.xfre.2023.11.012.
13. Mariya T, Shichiri Y, Sugimoto T, Kawamura R, Miyai S, Inagaki H, et al. Clinical application of long-read nanopore sequencing in a preimplantation genetic testing pre-clinical workup to identify the junction for complex Xq chromosome rearrangement-related disease. Prenat Diagn. 2023;43(3):304–13. https://doi.org/10.1002/pd.6334.
14. Gu S, Szafranski P, Akdemir ZC, Yuan B, Cooper ML, Magriñá MA, et al. Mechanisms for complex chromosomal insertions. PLoS Genet. 2016;12(11):e1006446. https://doi.org/10.1371/journal.pgen.1006446.
15. Kato T, Ouchi Y, Inagaki H, Makita Y, Mizuno S, Kajita M, et al. Genomic characterization of chromosomal insertions: insights into the mechanisms underlying chromothripsis. Cytogenet Genome Res. 2017;153(1):1–9. https://doi.org/10.1159/000481586.
16. Chiang C, Jacobsen JC, Ernst C, Hanscom C, Heilbut A, Blumenthal I, et al. Complex reorganization and predominant non-homologous repair following chromosomal breakage in karyotypically balanced germline rearrangements and transgenic integration. Nat Genet. 2012;44(4):390–7. https://doi.org/10.1038/ng.2202.
17. Sugimoto T, Inagaki H, Mariya T, Kawamura R, Taniguchi-Ikeda M, Mizuno S, et al. Breakpoints in complex chromosomal rearrangements correspond to transposase-accessible regions of DNA from mature sperm. Hum Genet. 2023;142(10):1451–60. https://doi.org/10.1007/s00439-023-02591-9.

Publisher's note